Use of Direct Microwave Irradiation in the Synthesis of Vanadium Phosphorus Oxide Catalysts via Vanadyl Hydrogen Phosphate Sesquihydrate Precursor

Jo Yee Kang[1], Loong Kong Leong[2,3*], Yeow Hong Yap[1], and Thian Khok Yong[1]

[1]*Lee Kong Chian Faculty of Science and Engineering, Universiti Tunku Abdul Rahman, Jalan Sungai Long, Bandar Sungai Long, Kajang, Selangor 43000, Malaysia*

[2]*Faculty of Engineering & Information Technology, Southern University College, PTD 64888, Jalan Selatan Utama, KM 15, Off, Skudai Lbh, Skudai 81300, Johor*

[3]*Excelube Marketing Sdn. Bhd., F-3A-17, IOI Boulevard, Jalan Kenari 5, Bandar Puchong Jaya, Puchong, Selangor 47170, Malaysia*

* ***Corresponding author:***

email: lkleong@sc.edu.my

Received: August 20, 2023
Accepted: November 13, 2023

DOI: 10.22146/ijc.88163

Abstract: *Four vanadyl pyrophosphate (VPO) catalysts were prepared via the sesquihydrate precursor route using direct microwave irradiation and reflux synthesis methods. The synthesis of the sesquihydrate precursor was carried out in 2 stages. The synthesized catalysts were denoted as VPOs-DD, VPOs-RR, VPOs-RD, and VPOs-DR; where VPOs represented VPO catalysts produced through sesquihydrate precursor, and D and R represented direct microwave irradiation and reflux synthesis methods, respectively. The direct microwave irradiation synthesis method was found to reduce the synthesis duration significantly for both stages of the precursor synthesis, from 48 to 4 h. An exclusive secondary configuration, akin to a needle-shaped form in chrysanthemums, is specifically noted in VPOs-DD could increase the specific surface area by 35.4% compared to the bulkier structure of VPOs catalyst produced via the conventional reflux synthesis method (VPOs-RR). Direct microwave irradiation could induce the removal of more than 4 times the total amount of oxygen atoms from the lattice of V^{4+} and V^{5+} phases, as compared to the conventional reflux method counterpart. This ultimately produced VPOs catalysts with greater catalytic performances and TON. In summary, employing direct microwave irradiation could generate VPOs catalysts with increased efficiency, improved activity and selectivity as compared to the conventional reflux method.*

Keywords: *direct microwave irradiation; sesquihydrate precursor; vanadium phosphorus oxide;* n*-butane oxidation*

■ INTRODUCTION

Light hydrocarbon, such as *n*-butane has gained significant attention throughout the world due to the mass production of maleic anhydride (MA). Such worldwide commercial application is highly essential for modern chemistry in reducing carbon dioxide emissions [1-9]. By selectively oxidizing *n*-butane, MA can be produced in a highly efficient and cost-effective manner. The exclusive focus on this process underscores its significance in the chemical industry and its role in the production of MA, a key component in the manufacturing of various products. The specific selective oxidation of *n*-butane using VPO catalyst has been extensively explored in the field of heterogeneous catalysis [10-27]. Vanadyl pyrophosphate (VPO) catalyst is the main focus of studies for the selective oxidation of *n*-butane to MA [28-39]. The primary characteristic of $(VO)_2P_2O_7$ lies in its capacity to demonstrate high selectivity in the activation of *n*-butane [40-44].

Significant endeavors have been made to enhance the catalytic capabilities of the VPO catalyst. Catalytic

characteristics and behavior of the VPO catalyst are greatly influenced by the preparation route and types of precursors, the synthesis method, the phosphorus to vanadium ratio, the calcination condition of the activation procedure, which includes temperature, duration and environment, dopant and/or support system used in the catalyst [45-50].

In general, the most effective catalyst precursor is $VOHPO_4{\cdot}0.5H_2O$, which transforms into $(VO)_2P_2O_7$ upon activation. However, the high yield of by-products of this catalyst remains a serious problem. The low activity from the conventional VPO catalyst has contributed to the issue of low supply and high demand of MA in the market. The existing reducing agent, benzyl alcohol, is a toxic compound that is harmful to the environment. Hence, a different pathway involving the vanadyl hydrogen phosphate sesquihydrate precursor was established by using 1-butanol as a reducing agent to convert $VOPO_4{\cdot}2H_2O$ into $VOHPO_4{\cdot}1.5H_2O$ precursor [40,51].

Microwave irradiation treatment facilitates a chemical reaction and has become a popular and promising technique in the scientific research community [52-56]. The advantages of applying microwave irradiation in the synthesis of catalysts could reduce the synthesis time and improve the catalytic performance [57]. This has allowed the synthesis of VPO catalysts to be simple, low-cost, and it demonstrates enhanced catalytic efficiency in the oxidation of *n*-butane to produce MA. The production of MA was noted to rise significantly, increasing from 21% with the conventional catalyst to 37% when using the VPO catalyst synthesized through microwave irradiation treatment [58]. In the microwave procedure, energy engages with substances on a molecular scale, creating internal electric fields. This capability leads to the transformation of electromagnetic energy into heat within the irradiated material [59-60].

The conventional reflux synthesis method requires a longer time to produce the VPO catalyst [51]. Therefore, microwave irradiation treatment is utilized to produce the catalyst precursor to shorten the duration of VPO catalyst production [61]. In previous research work, microwave irradiation was commonly used as an extra treatment for the VPO precursor synthesized via the conventional reflux synthesis method of VPO catalysts. Researchers found that the microwave irradiation treatment significantly reduced the reaction time required to synthesize VPO catalysts. This reduction in reaction time is attributed to the efficient heating provided by microwaves, which rapidly increases the temperature of the reaction mixture. Furthermore, the researchers observed that the microwave-assisted synthesis method resulted in higher product selectivity compared to the conventional method. The enhanced selectivity observed in microwave-assisted synthesis is believed to be due to the uniform and rapid heating provided by microwaves, which promotes the formation of the desired product [62-63].

A novel approach by utilizing microwave irradiation is introduced in this research as the primary synthesis method, bypassing the conventional reflux method. It also incorporates a modified chemical recipe ratio to address cost and time constraints while enhancing the comprehensive effectiveness of VPOs catalysts. The aim of this paper is to understand how microwave irradiation influences the performance of VPOs catalysts in terms of their physical and chemical attributes, as well as their reactivity and catalytic activity.

■ EXPERIMENTAL SECTION

Materials

The materials used in this study were V_2O_5 (≥ 98.0% purity, Merck), *o*-H_3PO_4 (85.0% purity, Merck), distilled water, 1-butanol (≥ 99.9% purity, Merck), and 0.75% *n*-butane in air mixtures (MOX).

Instrumentation

The instrumentations used in this study were Froilabo hotplate magnetic stirrer, microwave digester (Berghof Speedwave 4), XRD-6000 diffractometer (Shimadzu), Sorptomatic 1990 (Thermo Finnigan), optical emission spectrometer Optima 2000 DV (Perkin Elmer), S3400N scanning electron microscope (Hitachi) with EDAX software, TPDRO 1100 (Thermo Electron), and catalytic fixed-bed microreactor with online TRACE GC Ultra TM (Thermo Scientific).

Procedure

Catalyst preparation

VPOs catalysts were produced through a two-step method. In the initial stage, the vanadyl phosphate dihydrate ($VOPO_4{\cdot}2H_2O$) precursor was synthesized, involving two approaches: conventional reflux and direct microwave irradiation. For the reflux method, V_2O_5 (15 g) was mixed in a solution containing 90 mL of *o*-H_3PO_4 (85%) and 360 mL of deionized water. The mixture was subjected to stirring and refluxing at a temperature of 393 K for 24 h. In the direct microwave irradiation method, a combination of 15 g V_2O_5, 90 mL of *o*-H_3PO_4, and 360 mL of deionized water was placed in a Teflon-lined microwave vessel. The vessel underwent microwave irradiation for 2 h at 393 K using a microwave digestor at 2450 MHz and an output power of 850 W. The resulting yellow solid ($VOPO_4{\cdot}2H_2O$) from both synthesis methods in stage 1 was recovered by centrifugation and oven-dried for 24 h.

In stage 2, the $VOPO_4{\cdot}2H_2O$ obtained from both conventional reflux and direct microwave irradiation methods were each divided into two equal portions. The first portion (7.5 g) underwent reflux for 24 h with 1-butanol (116.5 mL), while the second portion was placed in a Teflon-lined microwave vessel with 7.5 g of $VOPO_4{\cdot}2H_2O$ and 116.5 mL of 1-butanol. The vessel was subjected to direct microwave irradiation for 2 h at 393 K using the same microwave digestor and parameters as in stage 1. The centrifugation process was employed to separate the resulting whitish-blue solids obtained from both synthesis methods in stage 2. These solids were then subjected to a 24 h drying period in an oven to remove any remaining moisture. The active VPOs catalysts were produced by calcining the acquired precursors in a reaction flow consisting of 0.75% *n*-butane in air mixtures at 733 K for 24 h. The synthesized catalysts were denoted as VPOs-DD, VPOs-RR, VPOs-RD, and VPOs-DR; where VPOs represented VPO catalysts produced through sesquihydrate precursor, and D and R represented direct microwave irradiation and reflux synthesis methods, respectively.

Catalysts characterization

The XRD technique was used with a Shimadzu model XRD-6000 diffractometer to obtain diffraction patterns of crystalline powder samples. Cu Kα radiation was used for this purpose, and the measurements were carried out at room temperature. The specific surface areas of the VPO catalysts were determined using the Brunauer-Emmett-Teller (BET) method. Nitrogen physisorption was performed at 77 K using the Thermo Finnigan Sorptomatic 1990 nitrogen adsorption-desorption analyzer.

The bulk chemical composition of VPOs catalysts was evaluated using the inductively coupled plasma-optical emission spectrometer (ICP-OES) analysis technique. Perkin Elmer optical emission spectrometer Optima 2000 DV was employed to conduct these analyses. The average oxidation number of vanadium (V_{AV}) within the VPO catalysts was determined via the redox titration method [64]. Secondary structure images were captured using a Hitachi S3400N SEM. Energy-dispersive X-ray (EDX) analyses were conducted using the EDAX software. Temperature programmed reduction (TPR) in H_2/N_2 was performed using the Thermo Electron TPDRO 1100 instrument, which was incorporated with a thermal conductivity detector (TCD).

A laboratory fixed-bed microreactor on a small scale was established to conduct the conversion of *n*-butane into MA through oxidation. The experimental conditions involved a gas hourly space velocity (GHSV) of 2400 h^{-1} at 673 K, using a VPO catalyst sample (250 mg) with a 1% *n*-butane and air mixture flowing through the reactor. The resulting gases released as products were directed into a Thermo Scientific TRACE GC Ultra TM gas chromatography through a heated metal pipeline for gaseous analysis. This analysis aimed to generate insights into the catalytic performance, including the activity and selectivity of the catalysts.

The conversion of *n*-butane into MA through oxidation was conducted in a fixed-bed microreactor at 673 K, maintaining a GHSV of 2400 h^{-1} and utilizing a standard catalyst mass (0.25 g) as depicted in Fig. 1. The

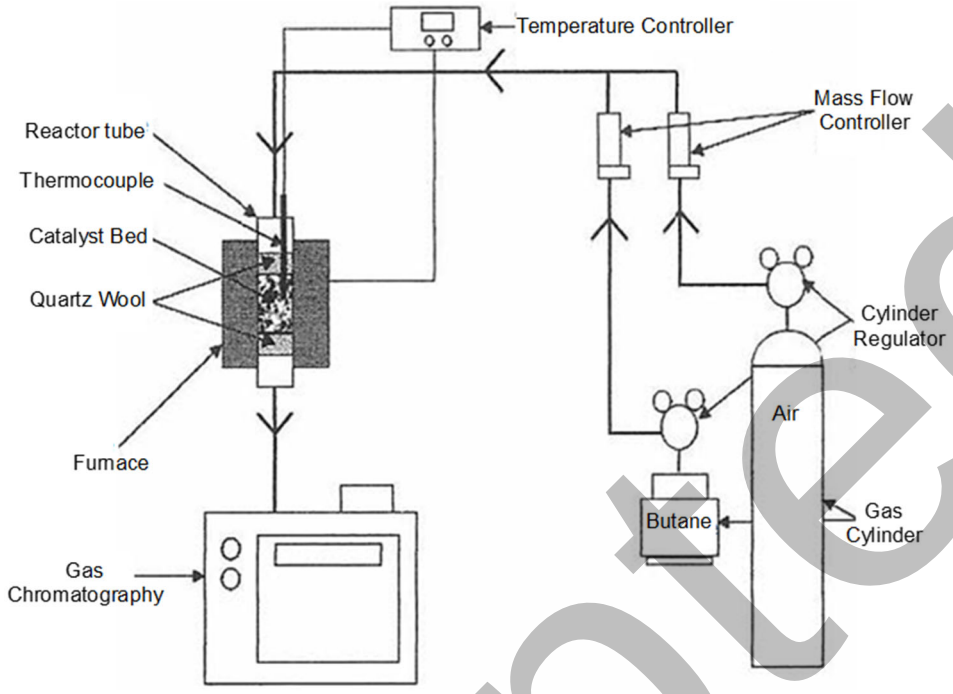

Fig 1. Laboratory scale fixed-bed microreactor with an online GC

catalyst was securely positioned using plugs of quartz wool. The reactor received a supply of a mixture consisting of *n*-butane and air, where the feedstock composition was 1% *n*-butane in air. This supply was carefully regulated using calibrated mass flow controllers. The product was transported through heated lines to an online gas chromatography instrument, specifically the Thermo Scientific TRACE GC Ultra™, for gaseous analysis. A volume of 0.5 mL was utilized for this purpose.

■ RESULTS AND DISCUSSION

X-ray diffraction (XRD)

VPOs catalysts synthesized via direct microwave irradiation and conventional oven reflux showed diffraction patterns comprising of well-crystallized $(VO)_2P_2O_7$ phase (Fig. 2). Three main characteristic peaks were observed at 2θ = 22.9, 28.4, and 29.9° were assigned to (0 2 0), (2 0 4), and (2 2 1) planes, respectively (JCPDS File No. 34-1381). Two V^{5+} phases were also found in the XRD profiles, i.e., β-$VOPO_4$ at 2θ = 21.3° (JCPDS File No. 27-0948) and α_{II}-$VOPO_4$ at 2θ= 25.3 and 29.3° (JCPDS File No. 34-1247) [40,51,62]. A comparative analysis of phase intensities among VPOs-DD, VPOs-RR, VPOs-RD, and VPOs-DR distinctly revealed the impact of direct microwave irradiation on the synthesis process. Notably, during stage 1 precursor synthesis, direct microwave irradiation could induce the formation of β-$VOPO_4$ and α_{II}-$VOPO_4$. The phase composition of VPOs-DD was characterized by prominent V^{4+} and V^{5+} peaks, underscoring the enhanced catalytic performances attributed to the direct microwave irradiation synthesis. As for VPOs-RR, VPOs-DR and VPOs-RD, the V^{5+} peak intensities were significantly less prominent than those of VPOs-DD. As a result, these VPOs catalysts were found to exhibit lower catalytic performances as compared to VPOs-DD. This correlation was further substantiated by the findings from the TPR in H_2/N_2 analyses and catalytic tests presented in this study.

The formula to calculate the crystallite sizes of (0 2 0) and (2 0 4) was given by the Debye-Scherrer equation (Eq. (1)).

$$t = \frac{0.89\lambda}{FWHM \times \cos\theta} \quad (1)$$

In the context of (h k l) phase, where t represents the crystallite size, λ denotes the X-ray wavelength of Cu Kα radiation, FWHM signifies the full width at half maximum of the characteristic peak, and θ is the diffraction angle for the phase. As per Debye-Scherrer's

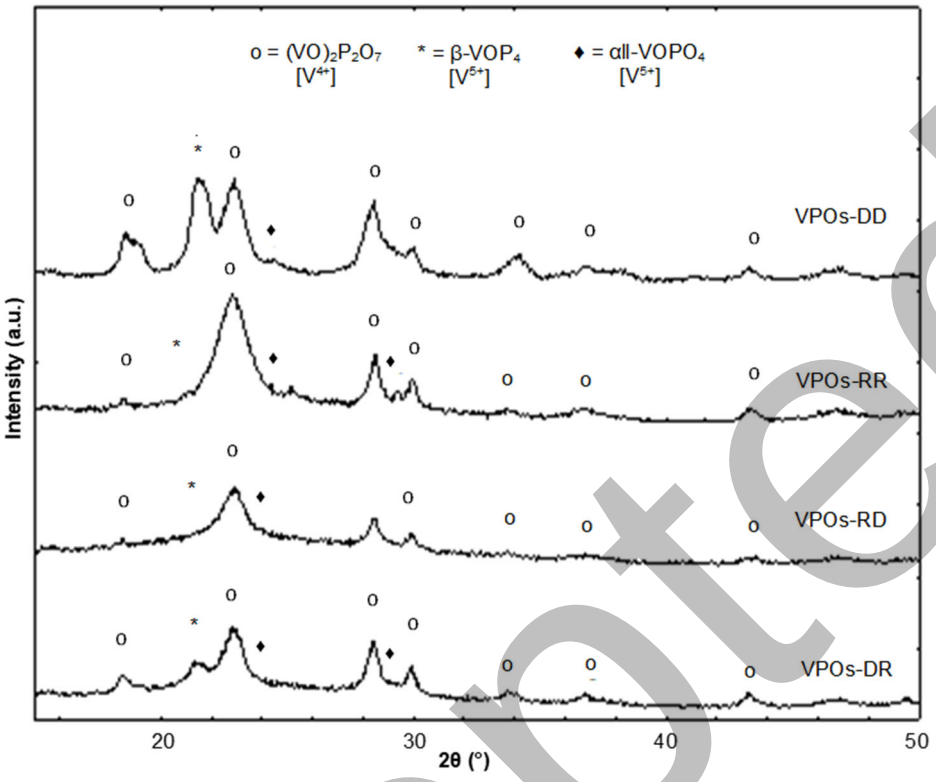

Fig 2. XRD profiles for VPOs catalysts

Table 1. XRD data for VPOs catalysts

Catalysts	Linewidth[a] (0 2 0) (°)	Linewidth[b] (2 0 4) (°)	Crystallite size[c] (0 2 0) (Å)	Crystallite size[c] (2 0 4) (Å)
VPOs-DD	0.9346	0.8945	86	122
VPOs-RR	1.4853	0.7180	54	113
VPOs-RD	1.2191	0.6871	66	118
VPOs-DR	1.0404	0.6620	77	129

[a] FWHM of (0 2 0) reflection plane; [b] FWHM of (2 0 4) reflection plane; [c] Crystallite size for (h k l) phase obtained by using Debye-Scherrer equation

equation, the crystallite size exhibits an inverse relationship with the FWHM of the reflection plane [65].

The determination of crystallite size in VPOs catalysts was carried out by analyzing the FWHM of the (0 2 0) and (2 0 4) reflection planes using XRD [65]. The resulting crystallite sizes for these planes across all VPOs catalysts were calculated and presented in Table 1. Interestingly, the adoption of direct microwave irradiation synthesis during the fabrication of VPOs catalysts yielded bigger crystallite sizes along the (0 2 0) and (2 0 4) reflection planes, in contrast to catalysts prepared through conventional reflux synthesis. This contrast has emphasized the impact of microwave irradiation in fostering a more pronounced surface morphology and contributed to an increase in the specific surface area of the catalysts.

BET Surface Area Measurements and Chemical Analyses

The specific surface areas of VPOs-DD, VPOs-RR, VPOs-RD and VPOs-DR were 24.38, 18.01, 17.52, and 21.02 $m^2 g^{-1}$, respectively (Table 2). It could be observed that VPOs catalyst synthesized by direct microwave irradiation (VPOs-DD) exhibited 35.4% higher specific surface area as compared to VPOs catalyst synthesized via conventional reflux counterpart (VPOs-RR). A similar

Table 2. BET surface areas measurements, chemical compositions and average oxidation number of vanadium for VPOs catalysts

Catalysts	Surface area (m^2/g)	P/V Atomic ratio (ICP-OES)	P/V Atomic ratio (EDX)	Average oxidation number of vanadium		
				V^{4+} (%)	V^{5+} (%)	V_{AV}
VPOs-DD	24.3800	1.2900	1.1400	47.7200	52.2800	4.5228
VPOs-RR	18.0100	1.2800	1.2600	36.1100	63.8900	4.6389
VPOs-RD	17.5200	1.2800	1.2400	57.1400	42.8600	4.4286
VPOs-DR	21.0200	1.2600	1.0100	76.2000	23.8000	4.2380

observation was also reported by Rownaghi and co-workers [57], whereby the VPO catalyst produced through the VPD route, incorporating microwave irradiation treatment, demonstrated an elevated specific surface area when contrasted with the VPO catalyst prepared solely through the reflux method [58]. Another pivotal observation concerning VPOs catalysts, synthesized through direct microwave irradiation in stage 1 (VPOs-DR and VPOs-DD) was their capability to manifest a comparatively elevated specific surface area in contrast to counterparts synthesized via reflux in stage 1 (VPOs-RD and VPOs-RR).

The above observations indicated that the improvement in the specific surface area of VPOs catalysts could only happen when the catalyst was prepared using the direct microwave irradiation synthesis method. This could be rationalized that the cavitation effect from direct microwave irradiation could increase the porosity and modify the structural morphology of VPOs catalyst platelets, which eventually led to the higher specific surface area.

Table 2 shows the P/V atomic ratio for all VPOs catalysts analyzed by using ICP-OES and EDX analyses. The P/V atomic ratio influences the distribution of these oxidation states, affecting the catalyst's ability to cycle between different oxidation states during the reaction. The proper redox behavior is necessary for maintaining catalytic activity over multiple reaction cycles. The P/V atomic ratio was observed to fall within the range of 1.01 to 1.29, which was quite close to the ideal atomic ratio range of P/V for generating an active and selective $(VO)_2P_2O_7$ phase, i.e., 1.0–1.2. The P/V atomic ratio surpassing unity signified that both direct microwave irradiation and reflux synthesis methods would induce phosphorus surface enrichment. This phenomenon could enhance the catalyst's ability to facilitate specific chemical transformations and increase the selectivity towards the desired products [66-67].

The percentages of V^{4+} and V^{5+} phases were determined by using the redox titration method [64] and were tabulated in Table 2. VPOs-DD exhibited the highest average oxidation state of vanadium among all VPOs catalysts. This observation has aligned well with the XRD analyses, which exhibited higher intensities in V^{5+} phases in the VPOs catalysts synthesized via direct microwave irradiation in both stages of precursor synthesis.

Secondary Electron Images by SEM

The secondary electron images of VPOs-DD, VPOs-RR, VPOs-RD and VPOs-DR catalysts (Fig. 3) showed rosette-shaped clusters consisting of crystal plates exhibiting varied forms and dimensions. These rosette-shaped clusters were deemed as the characteristic morphology of $(VO)_2P_2O_7$ catalysts that showed a preference for exposing the (1 0 0) reflection plane [67]. VPOs-RR exhibited the distinctive formation of rosette-shaped clusters, a trait recognized as indicative of VPOs catalyst synthesized through the sesquihydrate precursor [40]. However, the application of direct microwave irradiation could produce VPOs catalyst with chrysanthemum needle-like morphology with sharp edges and thinner crystal platelets compared to other VPOs catalysts. This distinctive feature could only manifest when the VPOs catalyst underwent direct microwave irradiation during both stages of precursor synthesis. This chrysanthemum needle-like played a substantial role in the increased specific surface area of VPOs catalyst as compared to conventional reflux synthesis counterparts, as evident in BET surface area

analyses. The growth of crystals is typically responsive to the initial nucleation phase. In the traditional reflux method, crystals tend to initiate on the walls of the container or impurity particles, resulting in a sluggish growth rate due to a limited number of nuclei. Conversely, when direct microwave irradiation was utilized in the creation of VPOs catalyst, the energy from microwave irradiation accelerated the nucleation rate, causing the rapid formation of numerous nuclei throughout the entire solution [68]. Microwave-assisted VPOs catalyst on either stage 1 and/or 2 exhibited smaller VPOs crystal platelets, as shown in SEM images of VPOs-DD, VPOs-RD and VPOs-DR as compared to VPOs-RR (Fig. 3).

TPR in H_2/N_2

TPR analysis in an H_2/N_2 atmosphere is employed to investigate the redox characteristics of VPO catalysts. This method provides additional insights into the nature and availability of oxidizing species from VPOs catalysts (O^-–V^{4+} and O^{2-}–V^{5+}). The TPR profiles for VPOs catalysts are illustrated in Fig. 4. Details such as peak maxima temperatures, the quantity of eliminated oxygen in each peak, and the resulting reduction activation energies can be found in Table 3. Three reduction peaks could be identified in TPR profiles for all VPOs catalysts synthesized via the sesquihydrate route and similar profiles could be observed in previous findings reported by Leong and co-workers [40]. The O^-–V^{4+} oxygen species was deemed as highly active in VPO to transform *n*-butane to MA, while the O^{2-}–V^{5+} species would contribute to the selectivity of this reaction [40,52].

VPOs-DD catalyst prepared via direct microwave-synthesized catalyst exhibited the removal of the highest total amount of oxygen atoms associated with both V^{4+} (O^-–V^{4+}) and V^{5+} (O^{2-}–V^{5+}) phases, i.e. 3.69×10^{21} atom g^{-1}. This significant value was found to be equivalent to more than 4 times the aggregate quantity of oxygen atoms extracted from the traditional reflux counterpart (VPOs-RR), i.e., 7.19×10^{20} atom g^{-1}. These results agreed well with the XRD analyses, where both V^{4+} and V^{5+} phases

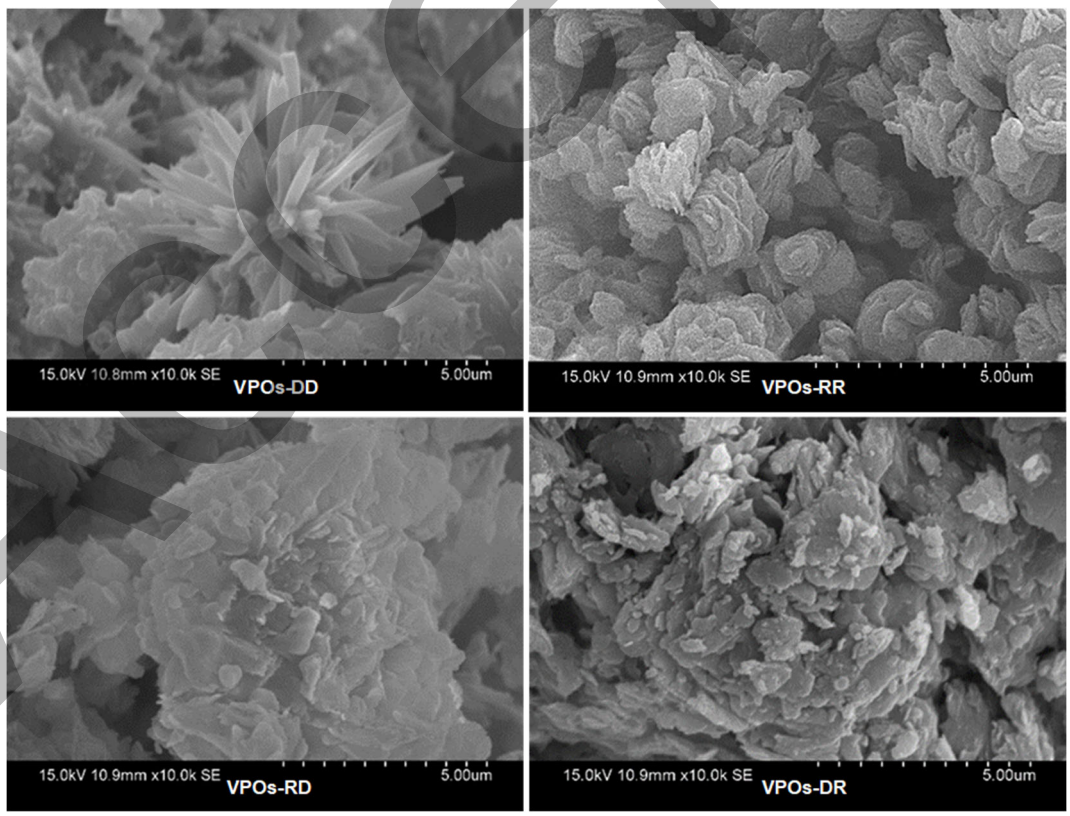

Fig 3. SEM micrographs for VPOs catalysts

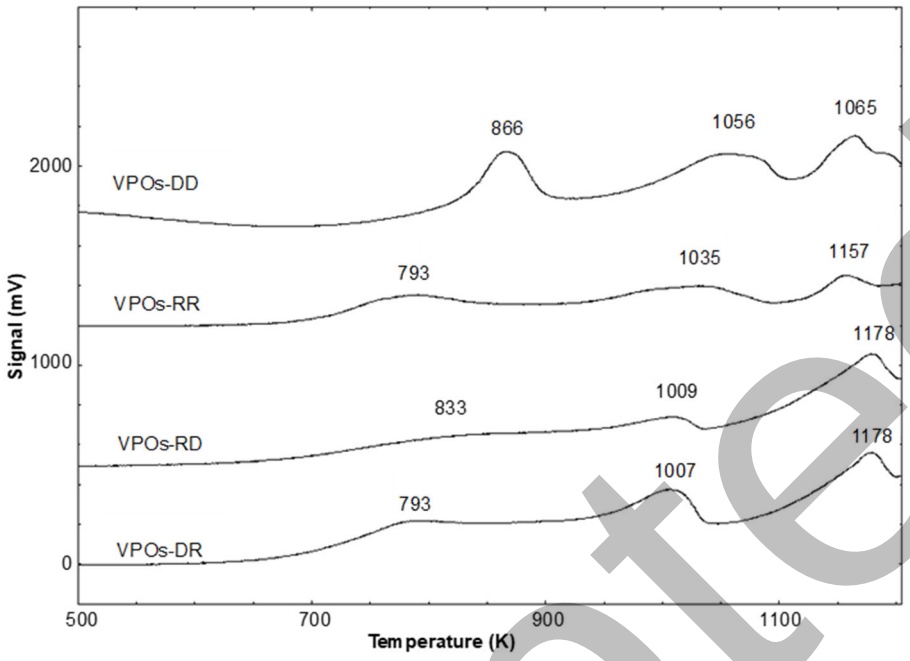

Fig 4. TPR in H_2/N_2 profiles for VPOs catalysts

Table 3. Total amount of oxygen atom, values of reduction activation energies obtained by the reduction in H_2/N_2 for VPOs catalysts

Catalysts	T_{max} (K)	Reduction activation energy E_r (kJ mol^{-1})	Oxygen atoms removed (mol g^{-1})	Oxygen atoms removed (atom g^{-1})
VPOs-DD	866	166.39	1.26×10^{-3}	7.59×10^{20}
	1056	202.90	2.77×10^{-3}	1.67×10^{21}
	1165	223.84	2.09×10^{-3}	1.26×10^{21}
		Total oxygen removed:	6.12×10^{-3}	3.69×10^{21}
VPOs-RR	857	164.66	1.28×10^{-4}	7.71×10^{19}
	1029	197.71	7.43×10^{-4}	4.47×10^{20}
	1166	224.03	3.24×10^{-4}	1.95×10^{20}
		Total oxygen removed:	1.20×10^{-3}	7.19×10^{20}
VPOs-RD	833	160.05	6.58×10^{-4}	3.96×10^{20}
	1009	193.87	1.00×10^{-3}	6.04×10^{20}
	1178	226.34	2.30×10^{-3}	1.39×10^{21}
		Total oxygen removed:	3.96×10^{-3}	2.39×10^{21}
VPOs-DR	793	152.37	1.66×10^{-3}	1.00×10^{21}
	1007	193.48	1.46×10^{-3}	8.79×10^{20}
	1178	226.34	1.83×10^{-3}	1.10×10^{21}
		Total oxygen removed:	4.95×10^{-3}	2.98×10^{21}

were found to be more prominent in VPOs-DD than in VPOs-RR. Furthermore, the formation of chrysanthemum needle-like morphology with the highest specific surface area contributed the greatest oxygen mobility in the lattice of VPOs-DD as compared to other VPOs catalysts (VPOs-RD, VPOs-DR and VPOs-RR) in this study.

It could also be evident that all VPOs catalysts prepared through the direct microwave irradiation synthesis method, either in stage 1 (VPOs-DR) or stage 2 (VPOs-RD), exhibited notable enhancements in the quantity of removed oxygen atoms compared to the conventional reflux synthesis method (VPOs-RR). The overall amounts of oxygen atoms eliminated from VPOs-RD and VPOs-DR were 2.39×10^{21} atom g^{-1} and 2.98×10^{21} atom g^{-1}, respectively, which were more than 2 and 3 times higher than VPOs-RR catalyst, respectively. This phenomenon has indicated that the direct microwave irradiation synthesis method could produce a VPO catalyst with greater catalytic performances which will be discussed in the next section.

The activation energy values are derived from the adapted form of the Redhead equation (Eq. (2)) [69],

$$\frac{E_r}{RT_m^{\,2}} = \left(\frac{A_r}{\beta}\right)[H_2]_m \exp\left(\frac{-E_r}{RT_m}\right) \quad (2)$$

where E_r is the reduction activation energy (kJ mol^{-1}), T_m (K) is the temperature of the peak maximum in the rate of H_2 consumption, A_r represents the pre-exponential term for reduction (cm^3 mol^{-1} s^{-1}), assigned the value of a standard collision number of 10^{13} cm^3 mol^{-1} s^{-1}, and $[H_2]_m$ denotes the gas phase concentration of hydrogen (mol cm^{-3}) at the peak maximum. The reduction activation energies for the VPOs-DD catalyst were computed for the peak maxima (Table 3): (i) 166.39 kJ mol^{-1} at 866 K, (ii) 202.90 kJ mol^{-1} at 1056 K, and (iii) 223.84 kJ mol^{-1} at 1165 K. For the VPOs-RR catalyst, the reduction activation energies were 164.66, 197.71, and 224.03 kJ mol^{-1} at 857, 1029, and 1166 K, respectively. For the VPOs-RD catalyst, the calculated reduction activation energies were 160.05, 193.87 and 226.34 kJ mol^{-1} at 833, 1003 and 1178 K, respectively. VPOs-DR catalyst exhibited relatively the same reduction activation energies as previous catalysts, i.e., 152.37, 193.48 and 226.34 kJ mol^{-1} at 793, 1007 and 1178 K, respectively.

n-Butane Conversion, Product Selectivity and Turnover Number of VPOs Catalysts

The catalytic efficacy of the VPOs catalysts in the oxidation of *n*-butane to MA was evaluated using a laboratory fixed-bed microreactor at 673 K, a conventional operating temperature for VPO catalysts. Comprehensive information on the catalytic performance data for all VPOs catalysts was outlined in Table 4. The efficiency in converting *n*-butane for VPOs-DD, VPOs-RR, VPOs-RD, and VPOs-DR were 34, 16, 19, and 23%, correspondingly, while the MA selectivity for these VPOs catalysts stood at 95, 59, 88, and 93%, respectively. Relative to the VPOs-RR catalyst, VPOs-DD exhibited notable enhancements in activity and selectivity, increasing by 18 and 36%, respectively. These findings aligned with the outcomes derived from BET surface area measurements and TPR in H_2/N_2 analyses, whereby direct microwave irradiation could produce VPOs catalyst with 35.4% higher specific surface area and more than 4 times higher removable oxygen atoms as compared to VPOs-RR catalyst. Furthermore, the same phenomenon could also be observed on VPOs catalysts prepared via the direct microwave irradiation synthesis method either in stage 1 (VPOs-DR) or stage 2 (VPOs-RD).

Table 4. Catalytic performances of VPOs catalysts

Catalyst	*n*-butane conversion (%)	Turnover number (TON)	Product selectivity (%)	
			MA	CO/CO_2
VPOs-DD	34.00	1.39	95.00	5.00
VPOs-RR	16.00	0.89	59.00	41.00
VPOs-RD	19.00	1.08	88.00	12.00
VPOs-DR	23.00	1.09	93.00	7.00

*Turnover number (TON) = $\frac{n-\text{butane conversion}}{\text{specific surface area (BET)}}$

Besides that, VPOs-DD catalyst showed the highest turnover number (TON), i.e. 1.39, as compared to the conventional reflux synthesis method (VPOs-RR), i.e., 0.89. VPOs-DR and VPOs-RD gave about the similar TON numbers of 1.09 and 1.08, respectively. These results indicated that the direct microwave irradiation synthesis method would generate VPOs catalyst with higher efficiency in the butane oxidation process.

■ CONCLUSION

Direct microwave irradiation showed a promising synthesis method in the preparation of VPOs catalyst (VPOs-DD) via sesquihydrate precursor. This synthesis method has produced VPOs catalyst with a distinctive secondary structure of chrysanthemum needle-like morphology, which could induce higher specific surface area and higher removable active and selective lattice oxygen as compared to the conventional reflux synthesis method (VPOs-RR). As a result, VPOs-DD could exhibit the highest activity (34%), selectivity (95%) and TON (1.39) for the process of transforming *n*-butane into MA. In addition, the sesquihydrate precursor synthesis duration could be notably reduced from 48 to 4 h through the application of direct microwave irradiation. Ultimately, the overall production cost of VPO catalysts will be lowered. Various output powers and direct microwave irradiation durations can be manipulated for future studies in synthesizing VPOs catalysts. The mechanistic transformation of VPOs precursor into VPOs catalysts can be analyzed when direct microwave irradiation is employed in the production of VPOs catalysts. The application of the direct microwave irradiation technique has limited the volume of the reducing agent, i.e. 1-butanol, as the pressure tends to build in the Teflon vessel. This limitation can be overcome by using a bigger capacity of both Teflon vessels and microwave instruments.

■ ACKNOWLEDGMENTS

Financial support from UTAR Research Fund (IPSR/RMC/UTARRF/2016-C2/L06) and Mr. Chia Song Hee (Director of RICA Marketing Sdn. Bhd.) were gratefully acknowledged.

■ CONFLICT OF INTEREST

All authors declare that they have no conflicts of interest.

■ AUTHOR CONTRIBUTIONS

Jo Yee Kang and Loong Kong Leong contributed to research design, formal analysis, and write the manuscript. Yeow Hong Yap and Thian Khok Yong supervised the project and contributed to the final version of the manuscript. All authors provided critical feedback and helped shape the research, analysis, and manuscript.

■ REFERENCES

[1] Faizan, M., Li, Y., Zhang, R., Wang, X., Song, P., and Liu, R., 2022, Progress of vanadium phosphorous oxide catalyst for *n*-butane selective oxidation, *Chin. J. Chem. Eng.*, 43, 297–315.

[2] Mahmoud, E., Watson, D.A., and Lobo, R.F., 2014, Renewable production of phthalic anhydride from biomass-derived furan and maleic anhydride, *Green Chem.*, 16 (1), 167–175.

[3] Chatzidimitriou, A., and Bond, J.Q., 2015, Oxidation of levulinic acid for the production of maleic anhydride: Breathing new life into biochemicals, *Green Chem.*, 17 (8), 4367–4376.

[4] Hundhausen, U., Kloeser, L., and Mai, C., 2015, Usability of maleic anhydride as wood modification agent for the production of medium density fibreboards (MDF), *Eur. J. Wood Wood Prod.*, 73 (3), 283–288.

[5] Hu, L.F., Zhang, C.J., Chen, D.J., Cao, X.H., Yang, J.L., and Zhang, X.H., 2020, Synthesis of high-molecular-weight maleic anhydride-based polyesters with enhanced properties, *ACS Appl. Polym. Mater.*, 2 (12), 5817–5823.

[6] Mangili, P.V., Junqueira, P.G., Santos, L.S., and Prata, D.M., 2019, Eco-efficiency and techno-economic analysis for maleic anhydride manufacturing processes, *Clean Technol. Environ. Policy*, 21 (5), 1073–1090.

[7] Ali, E., Al-haj Ali, M., Alhumaizi, K., and Elharbawi,

M., 2017, Optimal oxygen feeding policy to maximize the production of maleic anhydride in unsteady state fixed bed catalytic reactors, *J. King Saud Univ., Eng. Sci.*, 29 (3), 204–211.

[8] Ali, M.A.H., and Al-Humaizi, K., 2014, Maleic anhydride production in a cross-flow reactor: A comparative study, *Can. J. Chem. Eng.*, 92 (5), 876–883.

[9] Santander, P., Bravo, L., Pecchi, G., and Karelovic, A., 2020, The consequences of support identity on the oxidative conversion of furfural to maleic anhydride on vanadia catalysts, *Appl. Catal., A*, 595, 117513.

[10] Mokrane, E., Barama, S., Barama, A., Hamid Alhassan, F., Taufiq-Yap, Y.H., Messaoudi, H., Slyemi, S., and Pinard, L., 2017, Solid-phase and precipitation synthesis of Ti-pyrophosphate for the catalytic oxydehydrogenation of *n*-butane, *C. R. Chim.*, 20 (11-12), 1037–1046.

[11] Faizan, M., Li, Y., Wang, X., Song, P., Zhang, R., and Liu, R., 2023, Rare earth metal based DES assisted the VPO synthesis for *n*-butane selective oxidation toward maleic anhydride, *Green Energy Environ.*, 8 (6), 1737–1752.

[12] Nguyen Dinh, M.T., Nguyen, T.L., Phan, M.D., Nguyen Dinh, L., Truong, Q.D., and Bordes-Richard, E., 2019, Control of the crystal morphology of $VOHPO_4{\cdot}0.5H_2O$ precursors prepared via light alcohols-assisted solvothermal synthesis and influence on the selective oxidation of *n*-butane, *J. Catal.*, 377, 638–651.

[13] Shcherban, N.D., Diyuk, E.A., and Sydorchuk, V.V., 2019, Synthesis and catalytic activity of vanadium phosphorous oxides systems supported on silicon carbide for the selective oxidation of *n*-butane to maleic anhydride, *React. Kinet., Mech. Catal.*, 126 (2), 975–985.

[14] Schulz, C., Roy, S.C., Wittich, K., d'Alnoncourt, R.N., Linke, S., Strempel, V.E., Frank, B., Glaum, R., and Rosowski, F., 2019, α_{II}-$(V_{1-x}W_x)OPO_4$ catalysts for the selective oxidation of *n*-butane to maleic anhydride, *Catal. Today*, 333, 113–119.

[15] Trifirò, F., and Grasselli, R.K., 2014, How the yield of maleic anhydride in *n*-butane oxidation, using VPO catalysts, was improved over the years, *Top. Catal.*, 57 (14), 1188–1195.

[16] Wu, H.Y., Wang, H.B., Liu, X.H., Li, J.H., Yang, M.H., Huang, C.J., Weng, W.Z., and Wan, H.L., 2015, Samarium-modified vanadium phosphate catalyst for the selective oxidation of *n*-butane to maleic anhydride, *Appl. Surf. Sci.*, 351, 243–249.

[17] He, B., Nan, L., Li, Z., Wen, B., Niu, J., and Liu, R., 2019, Effect of Mo species on the selective oxidation of *n*-butane to maleic anhydride over Mo-promoted VPP, *ChemistrySelect*, 4 (2), 662–669.

[18] Eichelbaum, M., Glaum, R., Hävecker, M., Wittich, K., Heine, C., Schwarz, H., Dobner, C.K., Welker-Nieuwoudt, C., Trunschke, A., and Schlögl, R., 2013, Towards physical descriptors of active and selective catalysts for the oxidation of *n*-butane to maleic anhydride, *ChemCatChem*, 5 (8), 2318–2329.

[19] Shi, Y., Dai, F., Zhang, T., He, B., Zhang, R., Liu, R., and Ren, B., 2020, Hydroxyl-rich deep eutectic solvents assistant synthesis of VPO and its application in selective oxidation of *n*-butane, *ChemistrySelect*, 5 (23), 6907–6917.

[20] Cheng, M.J., Goddard, W.A., and Fu, R., 2014, The reduction-coupled oxo activation (ROA) mechanism responsible for the catalytic selective activation and functionalization of *n*-butane to maleic anhydride by vanadium phosphate oxide, *Top. Catal.*, 57 (14), 1171–1187.

[21] Carrero, C.A., Schloegl, R., Wachs, I.E., and Schomaecker, R., 2014, Critical literature review of the kinetics for the oxidative dehydrogenation of propane over well-defined supported vanadium oxide catalysts, *ACS Catal.*, 4 (10), 3357–3380.

[22] Dai, F., Shi, Y., Zhang, T., Faizan, M., Li, Z., Zhang, R., Liu, R., and Zhang, S., 2020, Phosphorus-based ionic liquid as dual function promoter oriented synthesis of efficient VPO catalyst for selective oxidation of n-butane, *Catal. Lett.*, 151 (1), 255–266.

[23] Novelli, M., Leonardi, M., and Cortelli, C., 2014, "Selective Oxidation Reactions in Polynt: An Overview of Processes and Catalysts for Maleic

Anhydride" in *Handbook of Advanced Methods and Processes in Oxidation Catalysis*, Imperial College Press, Covent Garden, London, UK, 334–352.

[24] Müller, M., Kutscherauer, M., Böcklein, S., Mestl, G., and Turek, T., 2020, On the importance of by-products in the kinetics of *n*-butane oxidation to maleic anhydride, *Chem. Eng. J.*, 401, 126016.

[25] Wilkinson, S.K., Simmons, M.J.H., Stitt, E.H., Baucherel, X., and Watson, M.J., 2013, A novel approach to understanding and modelling performance evolution of catalysts during their initial operation under reaction conditions – Case study of vanadium phosphorus oxides for *n*-butane selective oxidation, *J. Catal.*, 299, 249–260.

[26] Müller, M., Kutscherauer, M., Böcklein, S., Mestl, G., and Turek, T., 2021, Improved kinetics of *n*-butane oxidation to maleic anhydride: The role of byproducts, *Ind. Eng. Chem. Res.*, 60 (1), 218–229.

[27] Li, X., Ko, J., and Zhang, Y., 2018, Highly efficient gas-phase oxidation of renewable furfural to maleic anhydride over plate vanadium phosphorus oxide catalyst, *ChemSusChem*, 11 (3), 612–618.

[28] Kouvatas, C., Alonzo, V., Bataille, T., Le Pollès, L., Roiland, C., Louarn, G., and Le Fur, E., 2017, Synthesis, crystal structure of the ammonium vanadyl oxalatophosphite and its controlled conversion into catalytic vanadyl phosphates, *J. Solid State Chem.*, 253, 73–77.

[29] Schulz, C., Pohl, F., Driess, M., Glaum, R., Rosowski, F., and Frank, B., 2019, Selective oxidation of *n*-butane over vanadium phosphate based catalysts: Reaction network and kinetic analysis, *Ind. Eng. Chem. Res.*, 58 (7), 2492–2502.

[30] Lesser, D., Mestl, G., and Turek, T., 2016, Transient behavior of vanadyl pyrophosphate catalysts during the partial oxidation of *n*-butane in industrial-sized, fixed bed reactors, *Appl. Catal., A*, 510, 1–10.

[31] O'Leary, W.C., Goddard, W.A., and Cheng, M.J., 2017, Dual-phase mechanism for the catalytic conversion of *n*-butane to maleic anhydride by the vanadyl pyrophosphate heterogeneous catalyst, *J. Phys. Chem. C*, 121 (43), 24069–24076.

[32] Mestl, G., Lesser, D., and Turek, T., 2016, Optimum performance of vanadyl pyrophosphate catalysts, *Top. Catal.*, 59 (17), 1533–1544.

[33] Dai, F., Li, Z., Chen, X., He, B., Liu, R., and Zhang, S., 2018, Synthesis of vanadium phosphorus oxide catalysts promoted by iron-based ionic liquids and their catalytic performance in selective oxidation of *n*-butane, *Catal. Sci. Technol.*, 8 (17), 4515–4525.

[34] Caldarelli, A., Bañares, M.A., Cortelli, C., Luciani, S., and Cavani, F., 2014, An investigation on surface reactivity of Nb-doped vanadyl pyrophosphate catalysts by reactivity experiments and *in situ* Raman spectroscopy, *Catal. Sci. Technol.*, 4 (2), 419–427.

[35] Heine, C., Hävecker, M., Stotz, E., Rosowski, F., Knop-Gericke, A., Trunschke, A., Eichelbaum, M., and Schlögl, R., 2014, Ambient-pressure soft X-ray absorption spectroscopy of a catalyst surface in action: Closing the pressure gap in the selective *n*-butane oxidation over vanadyl pyrophosphate, *J. Phys. Chem. C*, 118 (35), 20405–20412.

[36] Bordes-Richard, E., 2021, Application of concepts in heterogeneous oxidation of hydrocarbons: Mo, V-based oxide catalysts for oxidation of ethane and of *n*- and *i*-butanes, *Catal. Today.*, 363, 15–26.

[37] Langeslay, R.R., Kaphan, D.M., Marshall, C.L., Stair, P.C., Sattelberger, A.P., and Delferro, M., 2019, Catalytic applications of vanadium: A mechanistic perspective, *Chem. Rev.*, 119 (4), 2128–2191.

[38] Wu, H.Y., Jin, P., Sun, Y., Yang, M.H., Huang, C.J., Weng, W.Z., and Wan, H.L., 2016, Enhancing catalytic performance of phosphorus-modified ceria supported VPO catalysts for *n*-butane oxidation, *J. Mol. Catal. A: Chem.*, 414, 1–8.

[39] Chu, W., Luo, J., Paul, S., Liu, Y., Khodakov, A., and Bordes, E., 2017, Synthesis and performance of vanadium-based catalysts for the selective oxidation of light alkanes, *Catal. Today*, 298, 145–157.

[40] Leong, L.K., Chin, K.S., and Taufiq-Yap, Y.H., 2012, Effect of varying reflux durations on the physico-chemical and catalytic performance of vanadium phosphate catalysts synthesized via vanadyl

hydrogen phosphate sesquihydrate, *Appl. Catal., A*, 415-416, 53–58.

[41] He, B., Li, Z., Zhang, H., Dai, F., Li, K., Liu, R., and Zhang, S., 2019, Synthesis of vanadium phosphorus oxide catalysts assisted by deep-eutectic solvents for *n*-butane selective oxidation, *Ind. Eng. Chem. Res.*, 58 (8), 2857–2867.

[42] Schulz, C., Kraehnert, R., Rosowski, F., and Frank, B., 2018, Selective oxidation of *n*-butane over vanadium-phosphorus oxide: Oxygen activation and dynamics, *ChemCatChem*, 10 (23), 5523–5532.

[43] Rezaei, M., Najafi Chermahini, A., and Dabbagh, H.A., 2017, Green and selective oxidation of cyclohexane over vanadium pyrophosphate supported on mesoporous KIT-6, *Chem. Eng. J.*, 314, 515–525.

[44] Feng, X., Yao, Y., Su, Q., Zhao, L., Jiang, W., Ji, W., and Au, C.T., 2015, Vanadium pyrophosphate oxides: The role of preparation chemistry in determining renewable acrolein production from glycerol dehydration, *Appl. Catal., B*, 164, 31–39.

[45] Palanychamy, P., Loong Kong, L., and Issabayeva, G., 2023, Effect of ultrasonic irradiation on the production of a dihydrate precursor for selective *n*-butane oxidation, *Mater. Today: Proc.*, In Press, Corrected Proof.

[46] Yang, D., Sararuk, C., Suzuki, K., Li, Z., and Li, C., 2016, Effect of calcination temperature on the catalytic activity of VPO for aldol condensation of acetic acid and formalin, *Chem. Eng. J.*, 300, 160–168.

[47] Böcklein, S., Mestl, G., Auras, S.V., and Wintterlin, J., 2017, On the correlation of structure and catalytic performance of VPO catalysts, *Top. Catal.*, 60 (19), 1682–1697.

[48] Mahdavi, V., and Hasheminasab, H.R., 2014, Vanadium phosphorus oxide catalyst promoted by cobalt doping for mild oxidation of benzyl alcohol to benzaldehyde in the liquid phase, *Appl. Catal., A*, 482, 189–197.

[49] Gu, Y., Liu, H., Yang, M., Ma, Z., Zhao, L., Xing, W., Wu, P., Liu, X., Mintova, S., Bai, P., and Yan, Z., 2020, Highly stable phosphine modified VO_x/Al_2O_3 catalyst in propane dehydrogenation, *Appl. Catal., B*, 274, 119089.

[50] Najari, S., Saeidi, S., Concepcion, P., Dionysiou, D.D., Bhargava, S.K., Lee, A.F., and Wilson, K., 2021, Oxidative dehydrogenation of ethane: Catalytic and mechanistic aspects and future trends, *Chem. Soc. Rev.*, 50 (7), 4564–4605.

[51] Ishimura, T., Sugiyama, S., and Hayashi, H., 2000, Vanadyl hydrogenphosphate sesquihydrate as a precursor for preparation of $(VO)_2P_2O_7$ and cobalt-incorporated catalysts, *J. Mol. Catal. A: Chem.*, 158 (2), 559–565.

[52] Taufiq-Yap, Y.H., Leong, L.K., Hussein, M.Z., Irmawati, R., and Abd Hamid, S.B., 2004, Synthesis and characterization of vanadyl pyrophosphate catalysts via vanadyl hydrogen phosphate sesquihydrate precursor, *Catal. Today*, 93-95, 715–722.

[53] Wang, Y., Zhuang, Q., and Ni, Y., 2015, Facile microwave-assisted solid-phase synthesis of highly fluorescent nitrogen-sulfur-codoped carbon quantum dots for cellular imaging, *Chem. - Eur. J.*, 21 (37), 13004–13011.

[54] Dąbrowska, S., Chudoba, T., Wojnarowicz, J., and Łojkowski, W., 2018, Current trends in the development of microwave reactors for the synthesis of nanomaterials in laboratories and industries: A review, *Crystals*, 8 (10), 379.

[55] Saggadi, H., Polaert, I., Luart, D., Len, C., and Estel, L., 2015, Microwaves under pressure for the continuous production of quinoline from glycerol, *Catal. Today*, 255, 66–74.

[56] Shaikh, S.P.S., Somalu, M.R., and Muchtar, A., 2016, Nanostructured Cu-CGO anodes fabricated using a microwave-assisted glycine–nitrate process, *J. Phys. Chem. Solids*, 98, 91–99.

[57] Rownaghi, A.A., Taufiq-Yap, Y.H., and Tang, J.W., 2009, Influence of the ethylene glycol, water treatment and microwave irradiation on the characteristics and performance of VPO catalysts for *n*-butane oxidation to maleic anhydride, *Catal. Lett.*, 130 (3), 593–603.

[58] Rownaghi, A.A., Taufiq-Yap, Y.H., and Rezaei, F., 2009, Solvothermal synthesis of vanadium phosphate catalysts for *n*-butane oxidation, *Chem. Eng. J.*, 155, 514–522.

[59] Horikoshi, S., Matsuzaki, S., Sakamoto, S., and Serpone, N., 2014, Efficient degassing of dissolved oxygen in aqueous media by microwave irradiation and the effect of microwaves on a reaction catalyzed by Wilkinson's catalyst, *Radiat. Phys. Chem.*, 97, 48–55.

[60] Horikoshi, S., and Serpone, N., 2014, On the influence of the microwaves' thermal and non-thermal effects in titania photoassisted reactions, *Catal. Today*, 224, 225–235.

[61] Sutradhar, M., Andrade, M.A., Carabineiro, S.A.C., Martins, L.M.D.R.S., Guedes da Silva, M.F.C., and Pombeiro, A.J.L., 2021. Oxido- and dioxido-vanadium(V) complexes supported on carbon materials: Reusable catalysts for the oxidation of cyclohexane, *Nanomaterials*, 11 (6), 1456.

[62] Chen, Z., Chen, Q., Wang, H., Zhang, R., Zhou, H., Chen, L., and Whittingham, M.S., 2014, A β-$VOPO_4$/ε-$VOPO_4$ composite Li-ion battery cathode, *Electrochem. Commun.*, 46, 67–70.

[63] Conde, L.D., Marún, C., Suib, S.L., and Fathi, Z., 2001, Frequency effects in the catalytic oligomerization of methane *via* microwave heating, *J. Catal.*, 204 (2), 324–332.

[64] Niwa, M., and Murakami, Y., 1982, Reaction mechanism of ammoxidation of toluene: IV. Oxidation state of vanadium oxide and its reactivity for toluene oxidation, *J. Catal.*, 76 (1), 9–16.

[65] Klug, P.H., and Alexander, L.E., 1974, *X-Ray Diffraction Procedures for Polycrystalline and Amorphous Materials*, 2nd Ed., Wiley-Interscience, New York, US.

[66] Cornaglia, L., Irusta, S., Lombardo, E.A., Durupty, M.C., and Volta, J.C., 2003, The beneficial effect of cobalt on VPO catalysts, *Catal. Today*, 78 (1-4), 291–301.

[67] Centi, G., 1993, Vanadyl pyrophosphate - A critical overview, *Catal. Today*, 16 (1), 5–26.

[68] Aït-Lachgar, K., Abon, M., and Volta, J.C., 1997, Selective oxidation of *n*-butane to maleic anhydride on vanadyl pyrophosphate: Influence of oxidation pretreatments on the catalytic performances, *J. Catal.*, 171 (2), 383–390.

[69] Redhead, P.A., 1962, Thermal desorption of gases, *Vacuum*, 12 (4), 203–211.